The second rainy season onset in the Central Highlands of Vietnam

Bui-Manh Hai[1], Chi-Ming Peng[1,2], Yen-Ta Fu[1], Duc-Tu Dinh[1,3], Neng-Huei Lin[1], and Ming-Cheng Yen[1]

[1]Department of Atmospheric Sciences, National Central University, Chung-Li, Taiwan.

[2] WeatherRisk Explore Inc., Taipei, Taiwan.

[3] Aero-Meteorological Observatory, Vietnam Meteorological and Hydrological Administration, Hanoi, Vietnam.

Corresponding author: Ming-Cheng Yen (tyenmc@atm.ncu.edu.tw)

Key Points:

- A second rainy season (SRS) is embedded within the conventional rainy season
- Early (late) SRS with a 1 month longer (shorter) rainfall period occurs in early July (until mid-August); a normal SRS starts in late July
- Almost all the early SRS years occur during El Niño developing phases

Abstract

Two distinct rainfall stages over the Central Highlands (CH) of Vietnam during the rainy season have been objectively defined using the high-resolution Vietnam Gridded Precipitation dataset for 1983–2010 (28 years): a second rainy season (SRS) embedded in the conventional rainy season. Surprisingly, the pronounced interannual variation in the SRS onset date has led to three apparent regimes: an early (late) SRS with a 1 month longer (shorter) rainfall period occurring in early July (until mid-August) and a normal SRS starting in late July. Almost all the early SRS years occur during El Niño developing phases, particularly during the Niño3.4 sea surface temperature (SST) increase from January through December. Water vapor budget analyses reveal that the interannual variation in the divergent water vapor flux is in response to the warmer July tropical Pacific SST anomalies, resulting in rainfall enhancement over the CH and eventually inducing early SRS onset.

Plain Language Summary

The Central Highlands (CH) of Vietnam contribute up to 90% of the country's total coffee production and 25% of its total hydropower potential. A second rainy season (SRS) is observed in late July in this region, which is distinct from the conventional rainy season that occurs in late April–early May. Because the onset of the SRS has a strong impact on coffee yield and hydropower potential in the CH, this study examines the climatology of and interannual variation in the SRS onset date during 1983–2010. An early (late) SRS with a 1 month longer (shorter) rainfall period occurs in early July (until mid-August). Almost all the early SRS years occur during El Niño developing phases. An association between the early SRS onset years and strengthening of the water vapor flux convergence induced by the warmer July tropical Pacific SST anomalies is discovered.

1 Introduction

An abrupt increase in rainfall during the monsoon season in Asia could have a strong impact on many activities of two thirds of the world's population, including agriculture, commerce, forestry, and hydropower. Over Southeast Asia, rapid precipitation enhancement mainly occurs during commencement of the Asian summer southwest monsoon, which signifies a transition from the dry to the rainy season (Lau & Yang, 1997; Zhang et al., 2002; Nguyen-Le et al., 2015). Therefore, research in past decades has increasingly focused on the summer monsoon onset date (SMOD) or summer rainy season onset date (RSOD). For example, Zhang et al. (2002) used the observed daily rainfall over the central Indochina Peninsula (ICP) to determine the mean SMOD as being 9 May, with a standard deviation of 12 days. Applying the empirical orthogonal function analysis on daily mean precipitation, Nguyen-Le et al. (2015) demonstrated that the mean summer RSOD over the eastern ICP is 6 May, with a standard deviation of 13 days. However, the immediate increase in rainfall over the eastern ICP is observed in early autumn when the summer monsoon withdraws (Matsumoto, 1997; Yen et al., 2011; Chen et al., 2012; Nguyen-Le et al., 2015).

Chen and Yoon (2000) demonstrated that the more (less) Indochina monsoon rainfall during cold (warm) summers is the result of global divergent water vapor flux following interannual variation in the global divergent circulation in response to tropical Pacific sea surface temperature (SST) anomalies. Numerous efforts have been made to explore the relationship between the interannual variation in monsoon onset and the El Niño Southern Oscillation

(ENSO). Years with cold (warm) SST anomalies in the equatorial central and eastern Pacific Ocean in the preceding spring tend to have a stronger (weaker) monsoon circulation and an early (late) SMOD and summer RSOD (Ju & Slingo, 1995; Zhang et al., 2002; Nguyen-Le et al., 2015; Noska & Misra, 2016). As revealed by previous studies (e.g., Yen et al., 2011; Chen et al., 2012), the maximum rainfall in coastal central Vietnam may undergo out-of-phase interannual variation with the ΔSST(Niño3.4) index during October–November. However, Nguyen-Le et al. (2015) illustrated that the mean autumn RSOD is 16 September, with a standard deviation of 12 days, and an early autumn RSOD was observed over the eastern ICP during the El Niño development phase. Nevertheless, Nguyen et al. (2007) argued that the precipitation in a small region of the Central Highlands (CH) of Vietnam is positively correlated with the equatorial central to eastern Pacific SST from July to September but has no significant relationship with the Indian Ocean SST.

The main coffee growing region of Vietnam, the second largest coffee producer worldwide (Amarasinghe et al., 2015), is located over the CH (green box in Figure 1a). Moreover, the hydropower potential generated from this region accounts for 25% of the country's total hydropower potential (Dao & Bui, 2015). Because rainfall variation significantly influences coffee production (Camargo, 2010) and hydropower potential, a thorough understanding of the RSOD and SMOD over the CH is crucial to both Vietnam's agriculture and economy. By using the same daily rainfall observations from 10 meteorological stations over the CH, Ngo-Thanh et al. (2018) found that the RSOD and SMOD are well differentiated from each other, with the mean RSOD being 20 April and SMOD being 13 May, whereas Pham-Thanh et al. (2020) demonstrated that the average RSOD was 28 April, with a standard deviation of 14 days, and that this was approximately 3 weeks before the mean SMOD in some years. Apart from the differing RSODs due to different determination criteria between them, both studies reported a strong correlation between the RSOD and the ENSO, but Pham-Thanh et al. (2020) reported most RSODs being later (earlier) during El Niño (La Niña) phases.

As revealed from the 5-day-running-mean climatology of the rainfall index averaged over the CH during May–October over the period 1983–2010 (Figure 1b), two distinct rainfall periods emerge: the first period fluctuates along a rainfall of 7.8 mm day^{-1} and the second vacillates at 10.4 mm day^{-1}. Hereafter, these two rainy periods are referred to as the first rainy season (FRS) and second rainy season (SRS), respectively. Studies related to rainfall over the CH have mostly focused on the RSOD (equivalent to the FRS onset date here: FRSOD; Ngo-Thanh et al., 2018; Pham-Thanh et al., 2020). To the best of our knowledge, this unique SRS feature and its onset date (SRSOD) have not previously been explored. Therefore, in this study, we objectively determine the SRSOD over the CH for the climatology as well as for each individual year during 1983–2010. In addition, the possible mechanism underlying the pronounced interannual variation in SRSOD is investigated.

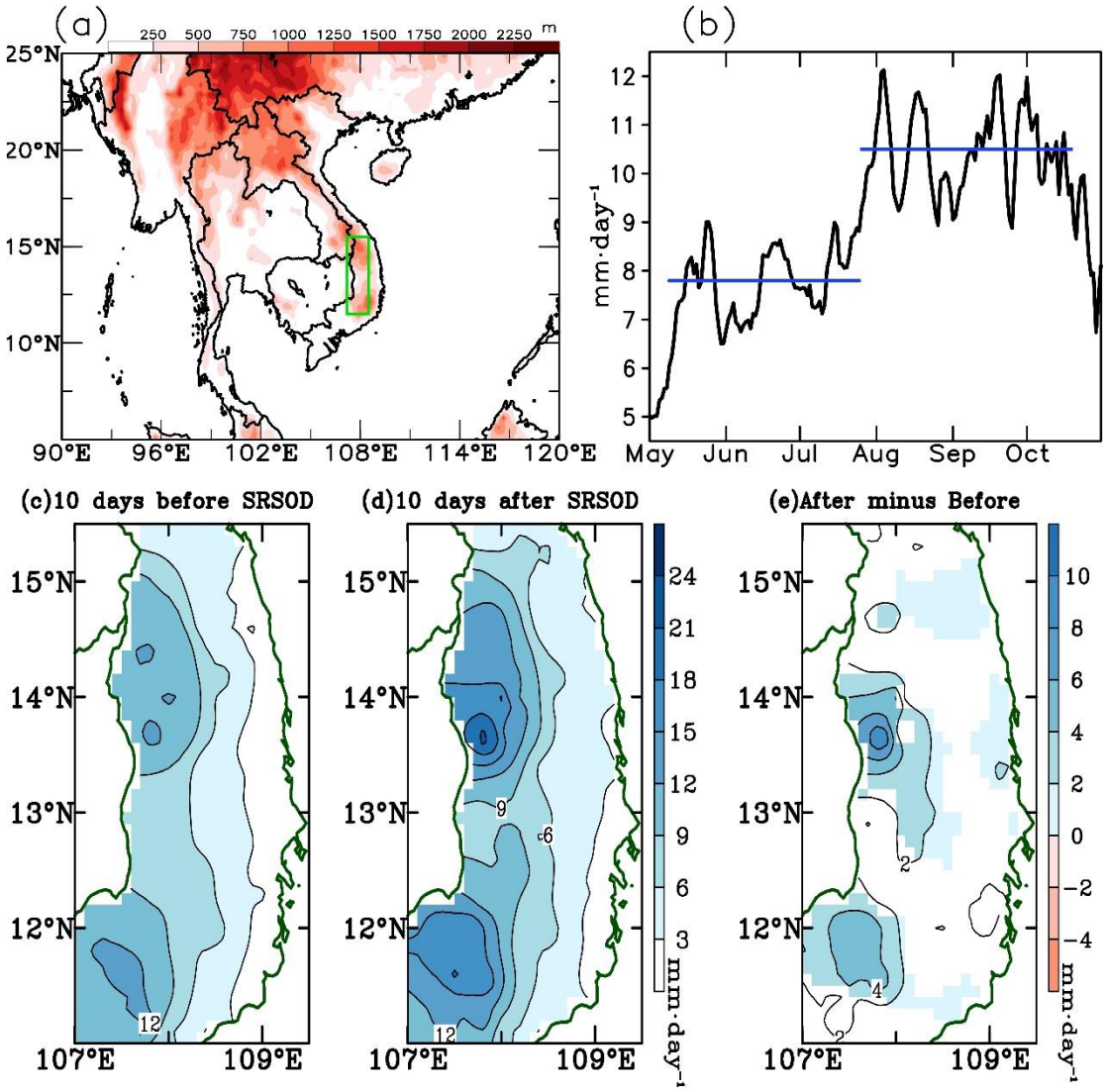

Figure 1. (a) Topography; green box indicates the CH. (b) Daily climatology (5-day-running mean) of the rainfall index averaged over the CH during May–October over the period 1983–2010; the two blue lines indicate the mean rainfall during the FRS (9 May–25 July) and SRS (26 July–20 October), respectively. Mean rainfall over central Vietnam during the 10 days (c) before and (d) after the SRSOD, including the SRSOD, and (e) their differences. Shaded areas in (e) indicate significant differences above 90% confidence level.

2 Data and Methods

2.1 Datasets

To investigate the spatial and temporal characteristics of precipitation on a scale relevant to the climate over the CH, two types of consistent, long-term, high-resolution gridded rainfall dataset are acquired. The first is the Vietnam Gridded Precipitation (VnGP) dataset with a high resolution of $0.1^o \times 0.1^o$ and generated from 481 daily raingauge observations across all Vietnam over the period 1980–2010 (Nguyen-Xuan et al., 2016). We use this dataset to construct the rainfall indices and investigate the local rainfall variability over the CH. The second dataset used

is the daily Precipitation Estimation from Remotely Sensed Information using Artificial Neural Networks for Climate Data Record (PERSIANN-CDR), which has a resolution of $0.25^o \times 0.25^o$ and is generated from long-term multisatellite high-resolution observations spanning 1983–2020 (Ashouri et al., 2015). This dataset is used to examine the relationship between rainfall variability in the CH and the surrounding activity embedded in the large-scale environment. To depict the large-scale atmospheric circulation associated with the SRSOD, daily ERA-Interim reanalysis on a 0.75^o latitude–longitude grid (Dee et al., 2011) is employed. Finally, the historical Oceanic Niño Index (ONI) provided by the Climate Prediction Center of National Centers for Environmental Prediction is adopted as a measure of the ENSO. For consistency, only the period 1983–2010 is covered in our analysis.

2.2 Definition of the second rainy season onset date

Because the SRS is a local feature in the CH and has not been observed in adjacent places, determination of the SRSOD by using only the rainfall parameter is proposed. In addition to the FRSOD and SRSOD, we designate RSRD and SRSRD as the rainy season retreat date and second rainy season retreat date, respectively. The procedures for detecting these four characteristic dates for the 28-year mean climatology are as follows:

1. FRSOD: The daily rainfall amount is larger than the yearly mean precipitation (PYRM) for 5 consecutive days. And, there must be at least 10 days with daily rainfall amount larger than the PYRM within 20 consecutive days after the FRSOD.
2. RSRD: The same constraint as for the FRSOD is used to determine the RSRD, but the estimation is done backward from the year end.
3. SRSRD: The procedure is similar to that for the RSRD, but the average precipitation during the period FRSOD–RSRD (PRSM: the average rainfall over the entire rainy season) is considered instead of the PYRM and backward estimation is conducted starting from the date calculated as the RSRD minus 10 days.
4. SRSOD: The same procedure as that for the FRSOD is used, but the PYRM is replaced by the PRSM.

The first two procedures are similar to those reported by Ngo-Thanh et al. (2018) except that the PYRM over 28 years is considered instead of directly specifying 5 mm day^{-1} as a reference level.

First, both temporal variation and rainfall magnitude, as shown in Figure 1b, are greatly consistent with the ground-truth rainfall index illustrated in Figure 2 of Pham-Thanh et al. (2020), suggesting that the VnGP dataset is suitable for climate research related to the CH. Consequently, two distinct rainy periods (Figure 1b and Table 1) are defined: the first fluctuates along the average rainfall of 7.8 mm day^{-1} from 9 May to 25 July, whereas the second vacillates at 10.4 mm day^{-1} from 26 July to 20 October. To further substantiate the clear temporal development, the average rainfalls for both the 10 days before and after the SRSOD together with their differences are depicted in Figures 1c–1e. The significant increase in precipitation after the SRSOD implies that our procedure is capable of reasonably identifying the SRSOD and capturing the two separate rainfall stages, the FRS and SRS, over the CH.

154

155 **Table 1.** Various rainy season dates and related average rainfall statistics

rainfall unit: mm day^{-1}				
Category	Climate	Early	Late	Normal
FRSOD	9 May	5 May	11 May	9 May
RSRD	21 Nov	5 Nov	27 Nov	28 Nov
SRSOD	26 Jul	7 Jul	19 Aug	26 Jul
SRSRD	20 Oct	7 Oct	22 Oct	4 Nov
Yearly rainfall average (PYRM)	5.7	5.9	5.6	5.7
Rainy season rainfall average (PRSM)	8.9	9.6	8.9	8.7
FRS rainfall average	7.8	7.1	7.6	7.7
SRS rainfall average	10.4	11.9	11.3	10.1

Onset date of the SRS over the CH from 1983 to 2010					
Year	SRSOD	Year	SRSOD	Year	SRSOD
1983	3 Aug	1993	26 Jul	2003	20 Jul
1984	27 Jul	1994	6 Jul	2004	23 Jul
1985	6 Aug	1995	19 Aug	2005	23 Jul
1986	15 Jul	1996	19 Jul	2006	29 Jun
1987	13 Aug	1997	10 Jul	2007	29 Jun
1988	11 Sep	1998	15 Aug	2008	22 Jul
1989	18 Jul	1999	23 Jul	2009	12 Jul
1990	13 Aug	2000	18 Aug	2010	22 Jul
1991	14 Aug	2001	3 Aug	**Average**	28 Jul

156

157 To reflect the apparent change in rainfall from the FRS to the SRS as well as the SRSOD
158 identification for each individual year, many sensitivity tests are performed to eventually obtain
159 the optimal criteria as follows. We first define some terms. P2SM denotes the average
160 precipitation during 9 May–20 October, a fixed period based on the climatological FRSOD–
161 SRSRD, for each individual year. PSA2 (PSB2) represents the average rainfall in the 20 days
162 after (before) the SRSOD including (excluding) the SRSOD. The SRSOD of the CH is then
163 determined by considering the first day after 27 June, just 1 month before 26 July of the
164 climatological SRSOD, which satisfied the following conditions:

165 1. The 5-day-moving-averaged daily rainfall amount exceeds P2SM and persists for at least 5
166 consecutive days.
167 2. PSA2 is greater than PSB2 + 0.35 × P2SM.

168 Consequently, the SRSODs for individual years during 1983–2010 are objectively determined
169 (Table 1), and they exhibit clear interannual variation. The average SRSOD for 28 years is 28
170 July, with a standard deviation of 17 days, whereas the earliest onset date is 29 June, occurred in
171 2006 and 2007, and the latest onset date is 11 September, 1998.

3 Results

Because of the wide distribution of SRSODs, investigating any specific characteristics among them is noteworthy. By using a standard deviation of ±0.8 of the SRSOD over 28 years as a measure, three discrete groups are selected and categorized as follows: early (1986, 1994, 1997, 2006, 2007, and 2009), late (1987, 1988, 1990, 1991, 1995, 1998, and 2000), and normal (other years) SRS. Additionally, the first three procedures mentioned in Section 2.2 are applied to the average rainfall index of each group to identify the FRSOD, RSRD, and SRSRD, whereas the SRSOD is simply calculated as the average of each group's onset dates. According to the statistics shown in Table 1 and Figure 2a, the early SRS years not only start earlier in terms of the FRSOD and SRSOD and end earlier in terms of the RSRD and SRSRD but also have a rainfall period 1 month longer than the late SRS years, along with higher precipitation in almost every epoch except the FRS. Coincidentally, both the FRSOD and SRSOD in normal years are identical to those in the 28-year climatology, with fewer rainfall differences for each rainy spell, which suggests that the 28-year climate mean might nearly reach the climatic norm with the exception of the RSRD and SRSRD. Although the FRSOD in each category is in early May, Pham-Thanh et al. (2020) stated that an RSOD over the CH between late April and early May seems to be more reasonable, not to mention using different criteria and datasets.

The intraseasonal oscillations (ISOs), including 10–20-day and 20–60-day modes, of the observed rainfall in Vietnam have been well documented by Truong and Tuan (2018, 2019), but these studies did not cover the CH. However, by using the VnGP dataset, Tuan (2019) found a remarkable relationship between the rainfall submonthly scale ISO and heavy rainfall days in the CH. Surprisingly, the SRSOD over the CH is synchronized with the developing phases of the 10–20-day and 20–60-day modes for each year in our study. Therefore, the original rainfall indices and their respective filtered ISO modes plus the combined ISOs for all the selected years in the aforementioned three groups are averaged with their center date coinciding with the SRSOD and extending 30 days before and after, as illustrated in Figures 2b–2d. In general, the precipitation clearly increases after the SRSOD in all three regimes, and the 10–20-day (20–60-day) mode is more dominant in early (late) SRS years, whereas these two ISO modes are compatible in the normal SRS years. These phenomena deserve extensive investigation in a future study.

To further substantiate the precipitous rainfall development over the CH during the transition from the FRS to the SRS, the composite rainfall, 28-year climate means with their center date coinciding with the SRSOD, evolution (Figures 2e–2i), and differences between two consecutive pentads (Figures 2j–2n) of pentad-mean VnGP (Text S1) are closely examined around the SRSOD. The prominent rainfall enhancement after the SRSOD is confirmed by the delineated physical domain with doubled rainfall intensity in Figure 2l if compared to that by the climate mean in Figure 1e.

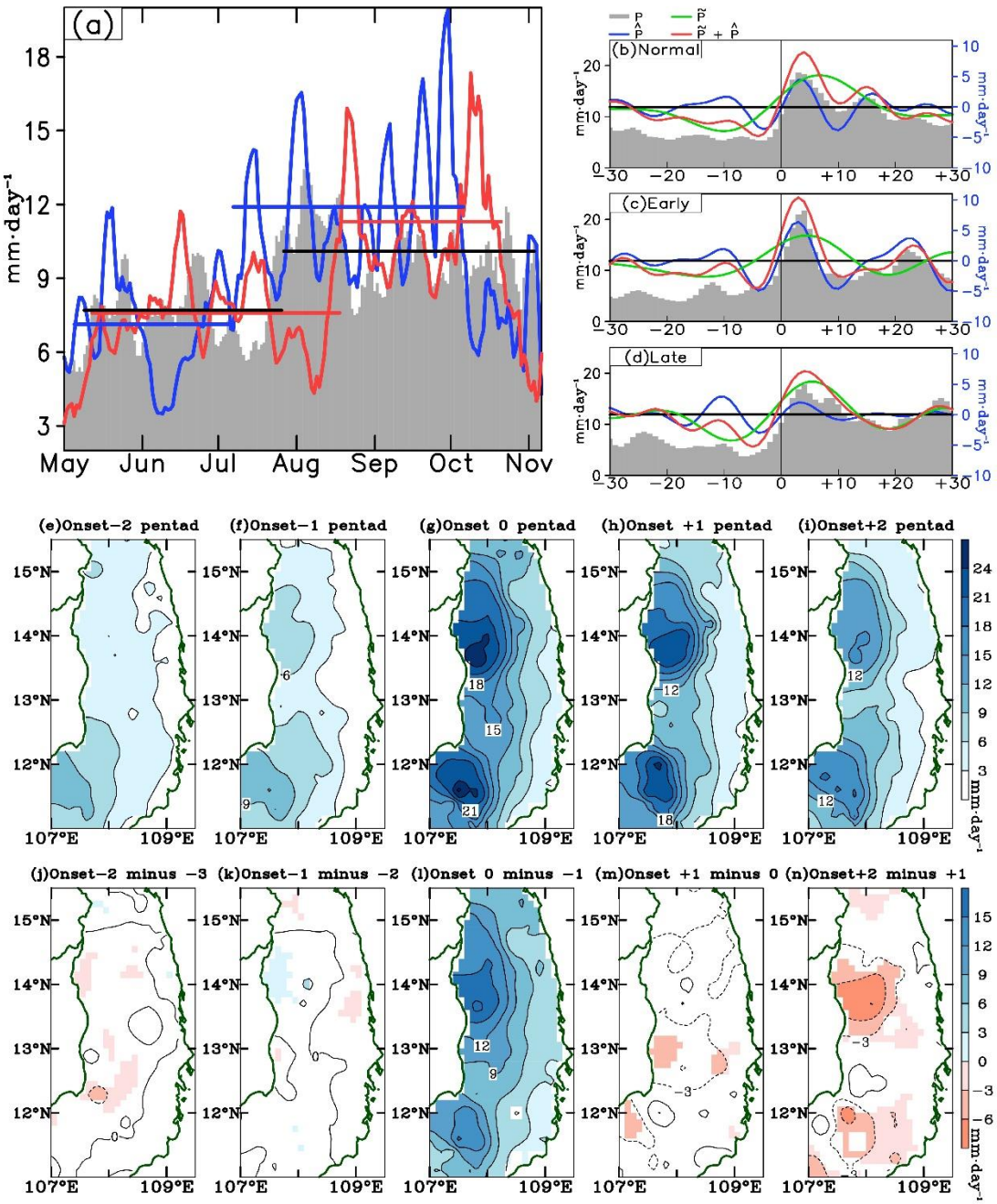

Figure 2. (a)Daily composite rainfall indices for normal (grey histogram), early (blue line), and late (red line) SRS years, respectively; two black, blue, and red horizontal lines indicate the rainfall mean during the FRS and the SRS for normal, early, and late SRS years, respectively. Daily evolution of composite P, $\tilde{P}$, $\hat{P}$, and $\tilde{P}$+$\hat{P}$ for (b) normal, (c) early, and (d) late SRS years; here $\tilde{P}$ and $\hat{P}$ represent the 20–60-day and 10–20-day modes, respectively. (e)–(i) Composite rainfall evolution and (j)–(n) differences between two consecutive pentads of pentad-mean VnGP over central Vietnam centered on the SRSOD. Shaded areas in (j)–(n) indicate a significant difference above 90% confidence level.

Regarding the conspicuous interannual variation in the SRSOD, July should be focalized on considering its critical role of water vapor budget (Text S2) in differentiating between the early and late SRS years because early (late) SRSODs occur in early July (until mid-August). The July composite charts of (ψ_Q, Q_R, W) and (χ_Q, Q_D, P) for normal, early, and late SRS years are displayed in Figures 3a–3f. In early SRS years, the abundant water vapor transported by strong westerly winds over south-southeast Asia and the strengthened southeasterly wind over northwestern Pacific (Text S3) is convergent toward the Philippine Sea west of 170°E and along the trough in the south fringe of the Asian Monsoon Low, including the CH. Furthermore, the significant increase in precipitation over these regions is accompanied and maintained by the enhancement of convergent water vapor flux (Figure 3d). By contrast, the phenomenon in the late SRS years associated with less vigorous water vapor transport and precipitation is similar to that in the normal years. These arguments are illustrated further in Figures 3g–3l. A couple of anomalous cyclonic cells of water vapor flux associated with the enhanced water vapor transport stretch from north India toward the Philippine Sea west of 170°E, covering the CH (Figure 3g), whereas the anomalous divergent water vapor flux $\Delta(\chi_Q, Q_D, P)$ converges water vapor toward these regions to maintain excessive rainfall (Figure 3h) in early SRS years. Evidently, the interannual rainfall variation in the CH is further ascertained by the composite rainfall differences (Figures 3i and 3l), confirming the decisive role of July composite charts in differentiating between early and late SRS years.

To explore the possible mechanism underlying the notable interannual variation in the SRSOD, the time series of ONIs for each selected year in the early and late onset categories is displayed in Figures 4a and 4b, respectively. Except for 2007, all early SRS years coincidently occur during El Niño developing phases, particularly with the Niño3.4 SST increase from January through December. Because of the developing effect of the tropical storm Toraji in early July, the persistent rainfall in the CH meets the SRSOD criteria despite the La Niña developing phase in 2007. For late SRS years, the large-scale environment appears to be considerably diverse and to comprise two El Niño (1987 and 1991), one normal (1990), one La Niña (2000), and three La Niña developing phases (1988, 1995, and 1998). This discrepancy in diversification warrants further investigation in the future.

An atypical Indian drought occurs during July 2002 with frequent advection of dry air from over the deserts instead of marine moist air from the southern Indian Ocean (Bhat, 2006) despite 2002 being one of the El Niño developing phase years. Consequently, the drier water vapor transport associated with divergence of water vapor flux replaces the moist large-scale environment over the CH to hinder the expected early SRS occurrence. On the basis of the distinct result shown in Figure 4a, the 5-year (except 2007) July composite chart of $\Delta(Q_D,$ SST) is constructed to support the interannual rainfall variation outcomes depicted in Figures 3g–3i. From Figure 4c, we can infer that the interannual variation in the divergent water vapor flux occurs in response to the warmer July tropical Pacific SST anomalies to enhance the rainfall over the CH and eventually induce early SRS onset.

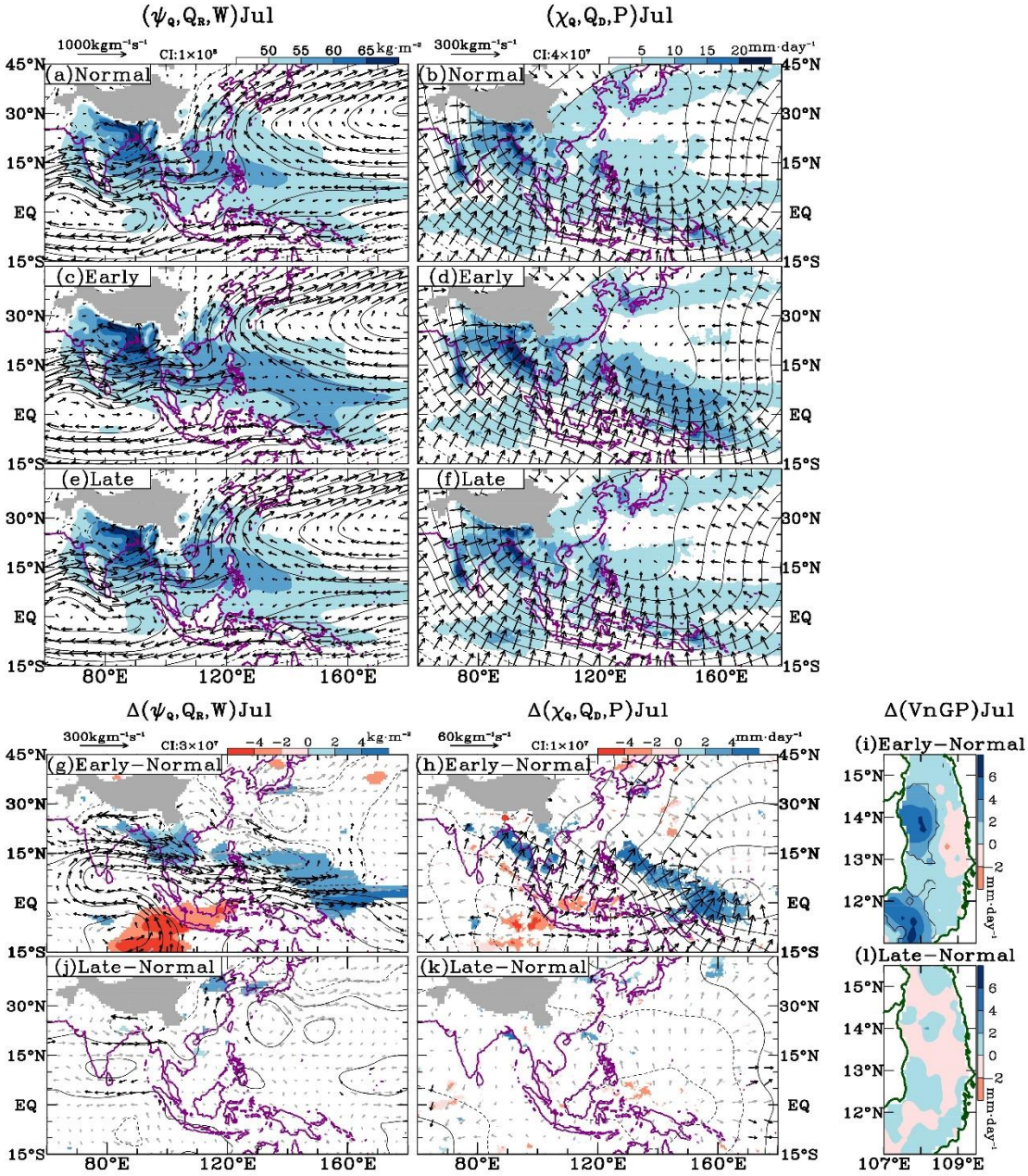

Figure 3. July composite charts of ψ_Q (contour), Q_R(vector), and W (shaded) for (a) normal, (c) early, and (e) late SRS years, respectively. (b), (d), (f) Same as (a), (c), and (e) except for χ_Q (contour), Q_D(vector), and P (shaded). July composite charts of $\Delta(\psi_Q, Q_R, W)$ for (g) early and (j) late SRS years. (h), (k) Same as (g) and (j) except for $\Delta(\chi_Q, Q_D, P)$; shaded areas and black vectors in (g), (h), (j), and (k) denote a significant difference above 90% confidence level. (i), (l) Same as (h) and (k) except for ΔVnGP; the areas that show a significant difference above 90% confidence level in (i) and (l) are encircled by solid-black contour.

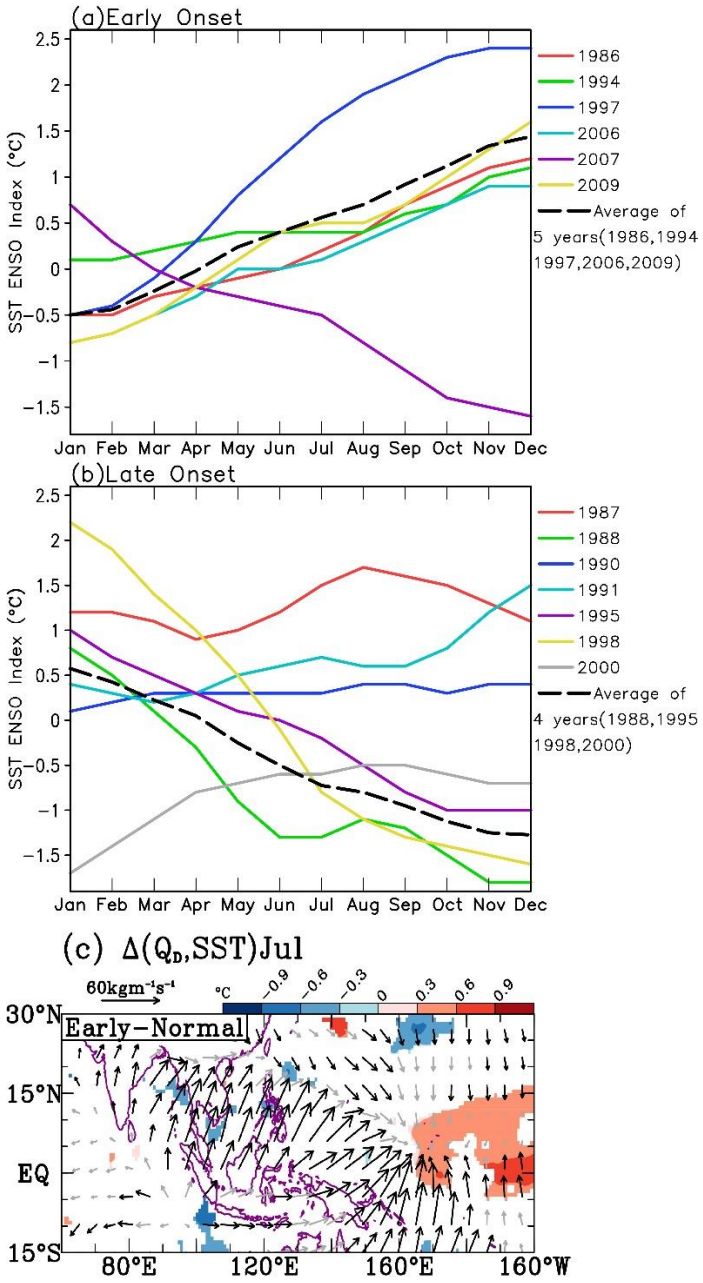

Figure 4. (a) Monthly SST of the ENSO index for six early SRS years and average of five El Niño years. (b) Same as (a) except for seven late onset years and average of four La Niña years. (c) July composite chart of $\Delta(Q_D, \mathrm{SST})$ in five El Niño years. Shaded areas and black vectors in (c) denote a significant difference above 90% confidence level.

4 Conclusions

The CH is a climatological subregion in Vietnam, and the region is the major production for second largest coffee producer worldwide while also having a quarter of the total hydropower potential of the country. Therefore, rainfall variation may affect coffee production and hydropower potential, thereby directly affecting the agricultural and economic gross in the CH and the entire country. The findings of this study are summarized as follows: By using the VnGP

dataset for the 1983–2010 period, two distinct rainy periods in the CH are identified; the first fluctuates along the average rainfall of 7.8 mm day^{-1} from 9 May (FRSOD) to 25 July, whereas the second vacillates at 10.4 mm day^{-1} from 26 July (SRSOD) to 20 October (SRSRD). However, the prominent year-to-year variation in SRSOD leads to three separate regimes: an early (late) SRS occurring in early July (until mid-August) and a normal SRS starting in late July. The early SRS years are characterized by higher precipitation with a 1 month longer rainfall period than the late SRS years. Except for two unusual years (2002 and 2007) during 1983–2010, all the early SRS years occur during El Niño developing phases, particularly with the Niño3.4 SST increase from January through December. The possible mechanism underlying the pronounced interannual variation in the SRSOD is inferred from water vapor budget analyses; the interannual variation in the divergent water vapor flux is in response to the warmer July tropical Pacific SST anomalies, resulting in rainfall intensification over the CH and eventually inducing early SRS onset.

Acknowledgments and Data

This study was supported by the Ministry of Science and Technology, Taiwan, under the grant MOST-108-2111-M-008-027. Data can be accessed online (VnGP:http://search.diasjp.net/en/dataset/VnGP_010; PERSIANN-CDR:https://www.ncei.noaa.gov/data/precipitation-persiann/access/; ERA-Interim:https://apps.ecmwf.int/datasets/data/interim-full-daily/levtype=sfc; ONI indices:https://origin.cpc.ncep.noaa.gov/products/analysis_monitoring/ensostuff/ONI_v5.php).

References

Amarasinghe, U. A., Hoanh, C. T., D'haeze, D., & Hung, T. Q. (2015). Toward sustainable coffee production in Vietnam: More coffee with less water. *Agricultural Systems*. *136*, 96-105. https://doi.org/10.1016/j.agsy.2015.02.008

Ashouri, H., Hsu, K.-L., Sorooshian, S., Braithwaite, D. K., Knapp, K. R., Cecil, L. D., et al. (2015). PERSIANN-CDR: Daily precipitation climate data record from multisatellite observations for hydrological and climate studies. *Bulletin of the American Meteorological Society, 96(1)*, 69-83. https://doi.org/10.1175/BAMS-D-13-00068.1

Bhat, G. S. (2006). The Indian drought of 2002 – a sub-seasonal phenomenon? *Quarterly Journal of the Royal Meteorological Society, 132*, 2583-2602. https://doi.org/10.1256/qj.05.13

Camargo, M. B. P. (2010). The impact of climatic variability and climate change on Arabic coffee crop in Brazil. *Bragantia, 69*, 239-247. https://doi.org/10.1590/S0006-87052010000100030

Chen, T.-C. (1985). Global water vapor flux and maintenance during FGGE. *Monthly Weather Review, 113***,** 1801–1819. https://doi.org/10.1175/1520-0493(1985)113<1801:GWV FAM >2.0.CO;2

Chen, T.-C., Tsay, J.-D., Yen, M.-C., & Matsumoto, J. (2012). Interannual variation of the late fall rainfall in central Vietnam. *Journal of Climate, 25(1)*, 392-413. https://doi.org/10.1175/JCLI-D-11-00068.1

Chen, T.-C., & Yoon, J.-H. (2000). Interannual variation in Indochina summer monsoon rainfall: possible mechanism. *J. Climate, 13(11)***,** 1979-1986. https://doi.org/10.1175/1520-0442(2000)013<1979:IVIISM>2.0.CO;2

Dao, N., & Bui, L. P. (2015). Rethinking Development Narratives of Hydropower in Vietnam. In *Hydropower Development in the Mekong Region: Political, Socio-economic and Environmental Perspectives*. (pp. 173-197). London: Earthscan.

Dee, D. P., Uppala, S., Simmons, A., Berrisford, P., Poli, P., Kobayashi, S., et al. (2011). The ERA-Interim reanalysis: Configuration and performance of the data assimilation system. *Quarterly Journal of the royal meteorological society, 137(656)*, 553-597. https://doi.org/10.1002/qj.828

Ju, J., & Slingo, J. (1995). The Asian summer monsoon and ENSO. *Quarterly Journal of the Royal Meteorological Society, 121(525)*, 1133-1168. https://doi.org/10.1002/qj.49712152509

Lau, K., & Yang, S. (1997). Climatology and interannual variability of the Southeast Asian summer monsoon. *Advances in Atmospheric Sciences, 14(2)*, 141-162. https://doi.org/10.1007/s00376-997-0016-y

Matsumoto, J. (1997). Seasonal transition of summer rainy season over Indochina and adjacent monsoon region. *Advances in Atmospheric Sciences, 14(2)*, 231-245. https://doi.org/10.1007/s00376-997-0022-0

Ngo-Thanh, H., Ngo-Duc, T., Nguyen-Hong, H., Baker, P., & Phan-Van, T. (2018). A distinction between summer rainy season and summer monsoon season over the Central Highlands of Vietnam. *Theoretical and applied climatology, 132*, 1237-1246. https://doi.org/10.1007/s00704-017-2178-6

Nguyen, T. D., Uvo, C., & Rosbjerg, D. (2007). Relationship between the tropical Pacific and Indian Ocean sea-surface temperature and monthly precipitation over the central highlands, Vietnam. *International Journal of Climatology, 27(11)*, 1439-1454. https://doi.org/10.1002/joc.1486

Nguyen-Le, D., Matsumoto, J., & Ngo-Duc, T. (2015). Onset of the rainy seasons in the eastern Indochina Peninsula. *Journal of Climate, 28(14)*, 5645-5666. https://doi.org/10.1175/JCLI-D-14-00373.1

Nguyen-Xuan, T., Ngo-Duc, T., Kamimera, H., Trinh-Tuan, L., Matsumoto, J., Inoue, T., & Phan-Van, T. (2016). The Vietnam Gridded Precipitation (VnGP) Dataset: Construction and Validation. *SOLA, 12*, 291-296. https://doi.org/10.2151/sola.2016-057

Noska, R., & Misra, V. (2016). Characterizing the onset and demise of the Indian summer monsoon. *Geophysical Research Letters, 43*, 4547-4554. https://doi.org/10.1002/2016GL068409

Pham-Thanh, H., van der Linden, R., Ngo-Duc, T., Nguyen-Dang, Q., Fink, A. H., & Phan-Van, T. (2020). Predictability of the rainy season onset date in Central Highlands of Vietnam. *International Journal of Climatology, 40(6)*, 3072–3086. https://doi.org/10.1002/joc.6383

Truong, N. M., & Tuan, B. M. (2018). Large-scale patterns and possible mechanisms of 10–20-day intra-seasonal oscillation of the observed rainfall in Vietnam. *International Journal of Climatology, 38(10)*, 3801-3821. https://doi.org/10.1002/joc.5534

Truong, N. M., & Tuan, B. M. (2019). Structures and Mechanisms of 20-60 day intraseasonal oscillation of the observed rainfall in Vietnam. *Journal of Climate, 32(16)*, 5191-5212. https://doi.org/10.1175/JCLI-D-18-0239.1

Tuan, B. M. (2019). Extratropical forcing of submonthly variations of rainfall in Vietnam. *Journal of Climate, 32(8)*, 2329-2348. https://doi.org/10.1175/JCLI-D-18-0453.1

Yen, M.-C., Chen, T.-C., Hu, H.-L., Tzeng, R.-Y., DINH, D. T., NGUYEN, T. T. T., & Wong, C. J. (2011). Interannual variation of the fall rainfall in Central Vietnam. *Journal of the Meteorological Society of Japan. Ser. II, 89*, 259-270. https://doi.org/10.2151/jmsj.2011-A16

370 Zhang, Y., Li, T., Wang, B., & Wu, G. (2002). Onset of the summer monsoon over the Indochina
371 Peninsula: Climatology and interannual variations. *Journal of Climate, 15(22)*,3206-3221.
372 https://doi.org/10.1175/1520-0442(2002)015<3206:OOTSMO>2.0.CO;2